Tidal Mixing Signatures in the Indonesian Seas*

AMY FFIELD

NOAA Atlantic Oceanographic and Meteorological Laboratory, Miami, Florida

ARNOLD L. GORDON

Lamont-Doherty Earth Observatory of Columbia University and Department of Geological Sciences, Columbia University, Palisades, New York

(Manuscript received 3 August 1995, in final form 19 March 1996)

ABSTRACT

Expressions of low-frequency tidal periods are found throughout the Indonesian Seas' temperature field, supporting the hypothesis that vertical mixing is enhanced within the Indonesian Seas by the tides. The thermal signatures of tidal mixing vary mostly at the fortnightly and monthly tidal periods due to nonlinear dynamics redistributing tidal energy into these periods. Away from the coasts, the largest tidal mixing signatures are observed in sea surface temperature within the Seram and Banda Seas. Most of the Indonesian Throughflow passes through the Banda Sea where strong vertical mixing modifies the thermocline by transferring surface heat and freshwater to deeper layers before the upper water column is exported to the Indian Ocean. Modulation of vertical eddy fluxes within the Indonesian Seas by fortnightly and monthly tides may act to regulate ocean–atmosphere fluxes.

1. Introduction

The earth's rotation is gradually slowing with a corresponding lengthening of the day; some of this planetary energy is dissipated by tidal mixing in the ocean through bottom friction, viscosity, the internal tide interacting with the internal wave continuum, and internal tides breaking (Cartwright and Ray 1989; Schott 1977). The Indonesian seas (Fig. 1) have been historically included in the regions shown to be major contributors to this energy loss because their extensive shelves, rough topography, and large tidal currents increase the potential for dissipation of tidal energy (Sjöberg and Stigebrandt 1992; Mihardja 1991; Miller 1966). The Indonesian Throughflow transports relatively warm, low salinity thermocline water from the western Pacific Ocean through the multitude of Indonesian seas and straits, to the Indian Ocean. Vertical mixing within the Indonesian seas significantly alters the thermohaline stratification and the velocity profile of the throughflow (Ffield and Gordon 1992; Gordon et al. 1994). For example, as the Indonesian Throughflow carries North Pacific thermocline water from the Sulawesi Sea to the Makassar Strait and Flores Sea, then to the Banda Sea and the Timor Sea, the salinity maximum at 100 db and salinity minimum at 300 db are greatly attenuated, presumably by mixing processes (Fig. 2). Using an advection–diffusion model and archived data, a relatively large vertical diffusivity coefficient is inferred for the Indonesian thermocline (K_z greater than 1×10^{-4} m^2 s^{-1}: Ffield and Gordon 1992). In general, the Indonesian thermocline is not conducive to salt fingers. However, any strong flows over the shallow shelves or through the narrow straits, or any high shears within the water column can contribute to the mixing in the region. The predicted high rates of regional tidal dissipation imply that tidal action is the source of enhanced mixing within the Indonesian seas. Dissipation of tidal energy occurs as tidal currents flow over the shelves, inducing turbulent mixing and, as tidal waves reflect from sloping topography, perturbing isopycnal surfaces and generating internal waves (internal tides) with large amplitudes and shear that can eventually break and mix (Sandstrom and Oakey 1995). As tidal energy is dissipated by mixing, the potential energy is increased within the interior of the seas. The continental shelf break in the Bay of Biscay (New 1988; New and Pingree 1990; Pingree and New 1991) and the Arctic pycnocline (Padman and Dillon 1991) are two examples of regions where the effect of tidal mixing has been studied. At some localities, tidal mixing can be as important as wind mixing: on the European shelf the energy dissipation from tidal

* Lamont-Doherty Earth Observatory Contribution Number 5523.

Corresponding author address: Amy Ffield, Lamont-Doherty Earth Observatory, Palisades, NY, 10964.
E-mail: affield@ldeo.columbia.edu

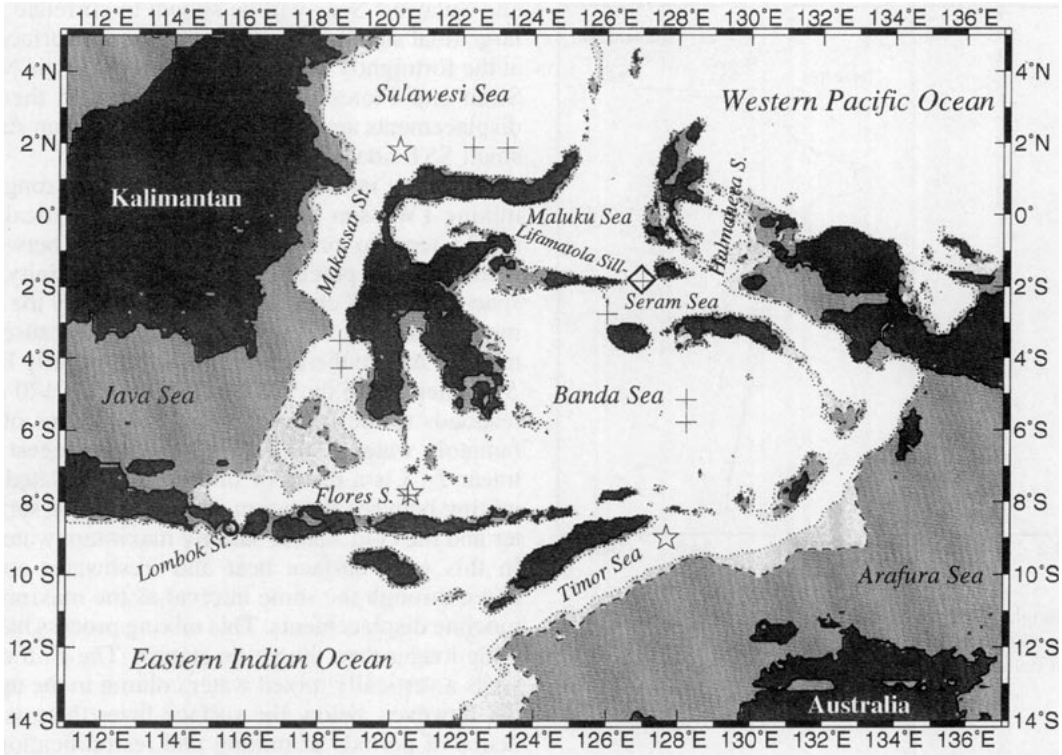

FIG. 1. Map of the Indonesian seas with bathymetry between 0 and 200 m shaded by dark gray and bathymetry between 200 and 500 m shaded by light gray. The locations of the ARLINDO Mixing CTD stations used in Fig. 2 are marked by stars, and the stations used in Fig. 3 are marked by crosses. The diamond shows the location of the Lifamatola Sill temperature and current meter used in Fig. 4, and the circle shows the location of the Lombok Strait pressure and temperature gauge used in Fig. 5.

mixing equals the energy dissipation from wind mixing if the maximum tidal amplitude is 0.5 m s^{-1} and if the wind speed is 13 m s^{-1} (Pingree et al. 1978).

In this paper four oceanographic time series datasets within the Indonesian seas are inspected for thermal signatures of tidal action to evaluate the hypothesis that vertical mixing is enhanced within the Indonesian seas by the tides. As none of these datasets were specifically designed to test this hypothesis, none form a definitive test. However, they all reveal some influence of low-frequency tides on the temperature values, and together should encourage more direct study of this potentially important phenomenon within the Indonesian Seas.

In the ocean the tidal forces are manifested by the rise and fall of sea level and currents with periodicities from hours to many years (Godin 1972; Pugh 1987). Because the tides are time dependent, their vertical mixing products will also be time dependent allowing them to be discerned within a time series by their periodicities (Loder and Garrett 1978). For example, tidal mixing can cool the sea surface temperature (SST) by mixing colder deeper water to the surface. Strong tidal mixing may be expected to depress the SST more than usual; weak tidal mixing less so. In section 2, CTD time series stations are used to demonstrate that the thermocline seems to oscillate at the semidiurnal tidal period in the Indonesian seas with associated vertical mixing. Section 3 reviews current meter and temperature data on the deep Lifamatola Sill, demonstrating that vigorous tidal phenomena also influence the deep Indonesian waters. In section 4, a shallow pressure and temperature record in the Lombok Strait is used to show that the thermal signature of tidal mixing varies at fortnightly and monthly tidal periods due to nonlinear dynamics redistributing tidal energy into these periods. In section 5, satellite-derived SST data reveal fortnightly and monthly tidal period oscillations throughout the Indonesian seas with the largest signals in the eastern seas.

2. ARLINDO mixing CTD data

The joint U.S. and Indonesian ARLINDO Mixing cruises in August–September 1993 and January–February 1994 measured the thermohaline characteristics throughout the Indonesian seas (Gordon 1995; Ilahude and Gordon 1996). The cruises included 209 CTD stations and 10 CTD time series (yo-yo stations) obtained during 14-h productivity stations (Fig. 1; Fig. 3).

In the ARLINDO Mixing CTD data the thermocline exhibited vertical excursions on the order of minutes

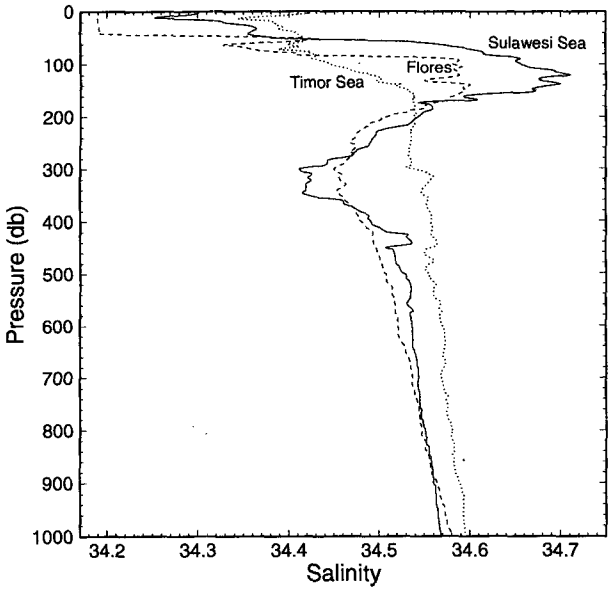

FIG. 2. Sample ARLINDO Mixing salinity profiles are shown for the Sulawesi Sea (solid line; 1.8°N, 120.3°E), Flores Sea (dotted line; 7.8°S, 120.6°E), and Timor Sea (dashed line; 9.0°S, 127.6°E).

and hours. Almost all the stations reveal some displacement during the down and up traces, probably due to internal waves. The isopycnal depths vary more over short timescales at specific stations than they do over the entire Indonesian seas. In addition, the yo-yo stations suggest that the thermocline oscillates over the semidiurnal period, probably due to internal tides. The Seram Sea and the Lifamatola Sill reveal the largest of these thermocline vertical displacements (Fig. 3). At the Lifamatola Sill the first cast (heavy line in Fig. 3) is vertically displaced upward in the upper thermocline, relative to the rest of the casts. Over the first 12 hours the profiles move down 70 db, then back up 70 db. Only the cast near the semidiurnal tidal period (dashed line, 12.8 h later) returns approximately to the same position as the first cast. At 14 hours, the last measured Lifamatola profile is displaced downward again.

The CTD yo-yo stations are undersampled over the 14 hours, nonetheless, the average maximum thermocline displacements of the available data are 30 db in the Makassar Sea, 35 db in the Flores Sea, 55 db in the Banda Sea, 60 db in the Sulawesi Sea, 70 db above the Lifamatola Sill, and 90 db in the Seram Sea (Fig. 3 and Table 1). In the Seram Sea and Lifamatola Sill the vertical displacements have a node at 150 m, probably due to internal tides rather than surface tides. Wunsch (1975) found the internal tidal signal to be intermittent either due to the character of the internal tides or increase in the background noise, and this could also influence the yo-yo time series as well as the poor sampling rate. However, in section 5 the appreciable thermocline oscillations in the Banda, Seram, Lifamatola, and Sulawesi Seas will be shown to correlate with the large tidal signals observed at the ocean surface in SST at the fortnightly and monthly periods. In the Makassar Strait and Flores Sea, the small vertical thermocline displacements are also reflected at the ocean surface by small SST tidal signals.

An active internal wave field implies strong vertical mixing (Wesson and Gregg 1994). Vertical mixing would tend to produce a straight line between end members in potential temperature–salinity (T–S) space. The T–S curves are not affected by the oscillating thermocline, unless those oscillations cause vertical mixing. Above the Lifamatola Sill the nearly linear T–S segment from the sea surface to 16°C (170 db) corresponds to the largest vertical oscillations of the Lifamatola water column (Fig. 3). We suggest that the linear T–S is a result of internal wave related vertical mixing between the warm, low salinity sea surface water and the cold, saltier salinity maximum water below. In this way, surface heat and freshwater are mixed down through the same interval as the maximum thermocline displacements. This mixing process has a timescale longer then the yo-yo station: The T–S curve reveals a vertically mixed water column in the upper 170 db, however, below the surface layer there is no evidence of periods of mixing and restratification during the 14-h sampling period. For all the yo-yo stations, the depth of most extreme linear portion of the T–S curve in the upper thermocline is used to estimate the interval mixed by the oscillating thermocline (Table 2). The average depths are 70 db in the Flores Sea, 110 db in the Makassar Strait, 128 db in the Sulawesi Sea, 170 db in the Lifamatola Sill, 170–230 db in the Seram Sea, and 200 db in the Banda Sea (Table 2). Again, the results will be shown to correlate with the tidal signatures observed in SST (section 5), with larger signatures in the eastern Indonesian Seas.

3. Lifamatola Sill current meter data

Strong tides and turbulent mixing are also observed in the deep Indonesian seas, demonstrating the prevalence of tidal phenomena in the Indonesian seas. During the joint Indonesian and Dutch *Snellius-II* 1985 expedition a mooring was deployed for 3 months at the Lifamatola Sill, the deepest connection between the Pacific Ocean and the Indonesian seas with a sill depth of 1940 m (see Fig. 1 for the mooring location). One hundred and sixty-three m over the sill the average flow was 0.61 m s^{-1} southeastward, filling the deep Seram and Banda Seas (Van Aken et al. 1988). The tides are primarily diurnal, and the velocities range from 0.2 to 1.2 m s^{-1} (Jonker et al. 1986). Over the 15 days selected from the *Snellius-II* record (Fig. 4), the daily low velocity was modulated at the fortnightly period with velocities ranging from 0.25 to 0.7 m s^{-1} with a corresponding fortnightly daily high temperature modulation of 3.75° to 3.2°C. (The mooring maintained its

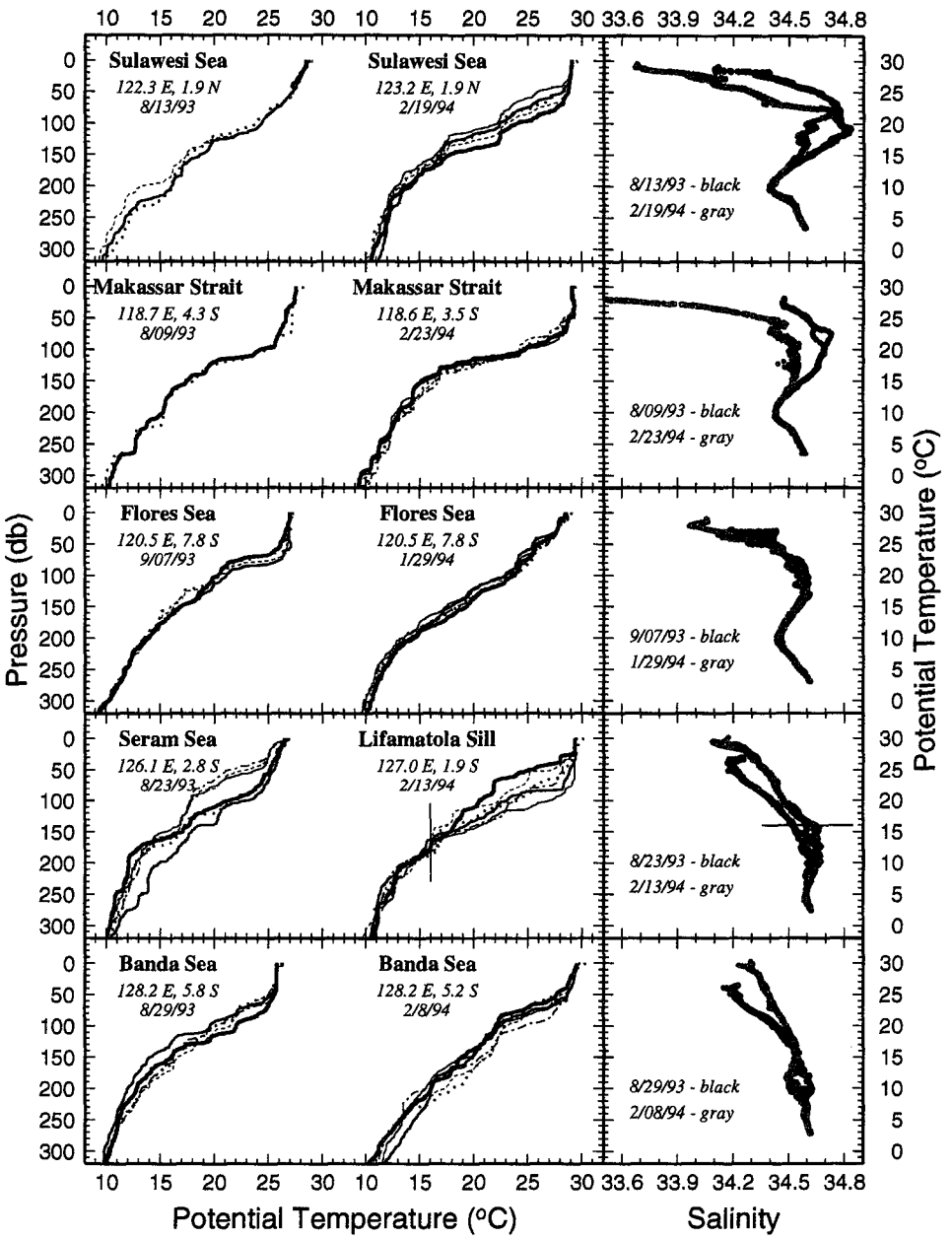

FIG. 3. Potential temperature profiles and potential temperature–salinity curves (T–S) of the ARLINDO Mixing 14-h CTD yo-yo stations. For the potential temperature profiles the thickest line is used for the first cast of the yo-yo station, the rest of the casts are distributed somewhat evenly over the remaining 14 h and are drawn in temporal order with a medium thick line, thin line, dashed–dotted line, dashed line, and dotted line (always the last cast of the yo-yo station). The line at 16°C on the Lifamatola Sill potential temperature profile marks the lower boundary of the maximum thermocline excursions, and on the corresponding T–S curve, a 16°C line marks the lower boundary of the well vertically mixed surface to 16°C interval.

target depth of 1777 m only when the velocities were low. Consequently only the low velocity values and the corresponding high temperatures are accurate measurements.) In addition, during the 1976 INDOPAC expedition for 28 days current meters at the Lifamatola Sill measured high-frequency flows with periodicities near 6, 8, 12, and 24 h that were attributed to baroclinic tidal currents (Broecker et al. 1986). Part of the temperature signal observed in Fig. 4 may represent tidal sloshing of a horizontal temperature gradient. However, temperature sections through the Lifamatola Sill demonstrate that turbulent mixing up to 500 m over the sill

TABLE 1. Maximum vertical isotherm displacements in the upper thermocline of the water column during the 14-h CTD yo-yo stations (Fig. 3). Units are decibars.

	Flores	Makassar	Sulawesi	Lifamatola	Seram	Banda
Aug–Sep 1993	30	—	50	—	90	55
Jan–Feb 1994	40	30	70	70	—	55
Average	35	30	60	80		55

increases the average temperature filling the Seram and Banda Seas (Broecker et al. 1986; Van Aken et al. 1988). If the flow over the Lifamatola Sill were laminar, the potential temperature at 3000 db in the Banda Sea would be near the sill potential temperature of about 2.2°C, rather than the observed 2.85°C. Therefore, the turbulent tidal mixing has the effect of increasing the heat stored in the deep Seram and Banda Seas.

4. Lombok Strait pressure and temperature data

A 1985 shallow pressure and temperature record on the shelf in the Lombok Strait (Murray and Arief 1990) is examined for tidal mixing signatures (see Fig. 1 for the location of the gauge). The time series is averaged to 14-min resolution, and 130 days of the series are plotted in Figs. 3a and 3d. The tide gauge pressure minus atmospheric pressure is equal to the sea level height above the gauge at these shallow depths. The numerous tidal components composing the pressure signal—all with different amplitudes, periods, and phases—add constructively (destructively) increasing (decreasing) the total ocean tide actually observed in Fig. 5a. In this way, for example, the M_2 and S_2 semidiurnal tides combine to produce a fortnightly (14.8 days) modulation, and the M_2 and N_2 semidiurnal tides combine to produce a monthly (27.6 days) modulation. Over a fortnight the sea level range at the Lombok Strait gauge is about 1 m during neap tides and 3 m during spring tides, and over a month the range of the two spring tides differs by about 1 m. Spectral analysis of the pressure time series reveals the semidiurnal and diurnal tidal periods within the time series, but not the periods at which they beat together (Fig. 6a).

The Lombok Strait pressure time series smoothed by a 7-day Gaussian filter overlays the 14-min data in Fig. 5a. The diurnal, semidiurnal, and shallow water tides

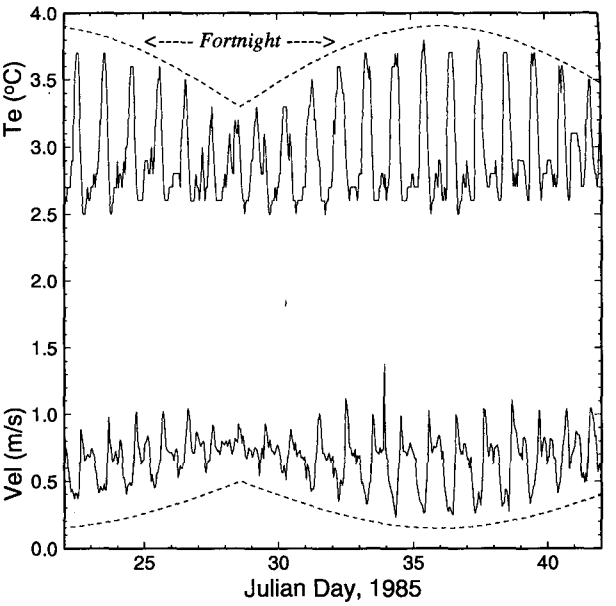

FIG. 4. A portion of the Lifamatola Sill temperature and velocity time series from the *Snellius-II* expedition (Jonker et al. 1986). The sill is 1940 m deep at the mooring (1.8°S, 127.0°E). The mooring maintained its target depth of 1777 m only when the velocities were low. Consequently only the low velocity values and the corresponding high temperatures are accurate measurements.

are removed by the weekly filter, and therefore their modulations are also eliminated. The filtered time series does not have any significant oscillations, and is essentially just the mean pressure value. In the temperature record (Fig. 5d) the weekly filter also removes higher frequency oscillations of about 3°C range associated with the tides. However, there are longer period oscillations remaining in the record: From day 60 to 74 and from day 104 to 118 the observed temperatures appear to follow a fortnightly cycle with a range of about 3°C. Spectral analysis of the temperature time series reveals semidiurnal, diurnal, and fortnightly tidal periods as well as peaks at 23 and 45 days (Fig. 6b). The fortnightly tidal period observed in the temperature record cannot be a linear modulation of the diurnal or semidiurnal tides. Two simple parameterizations are used to visualize the possible temperature changes produced by tidal currents, and the results are compared to the observed Lombok Strait temperature record.

TABLE 2. Depth of the most extreme linear portion of the potential temperature–salinity curve in the upper thermocline of the 14-h CTD yo-yo stations (Fig. 3). Units are decibars.

	Flores	Makassar	Sulawesi	Lifamatola	Seram	Banda
Aug–Sep 1993	—	110	140	—	170–230	180–220
Jan–Feb 1994	70	110	100–130	170	—	200
Average	70	110	128	185		200

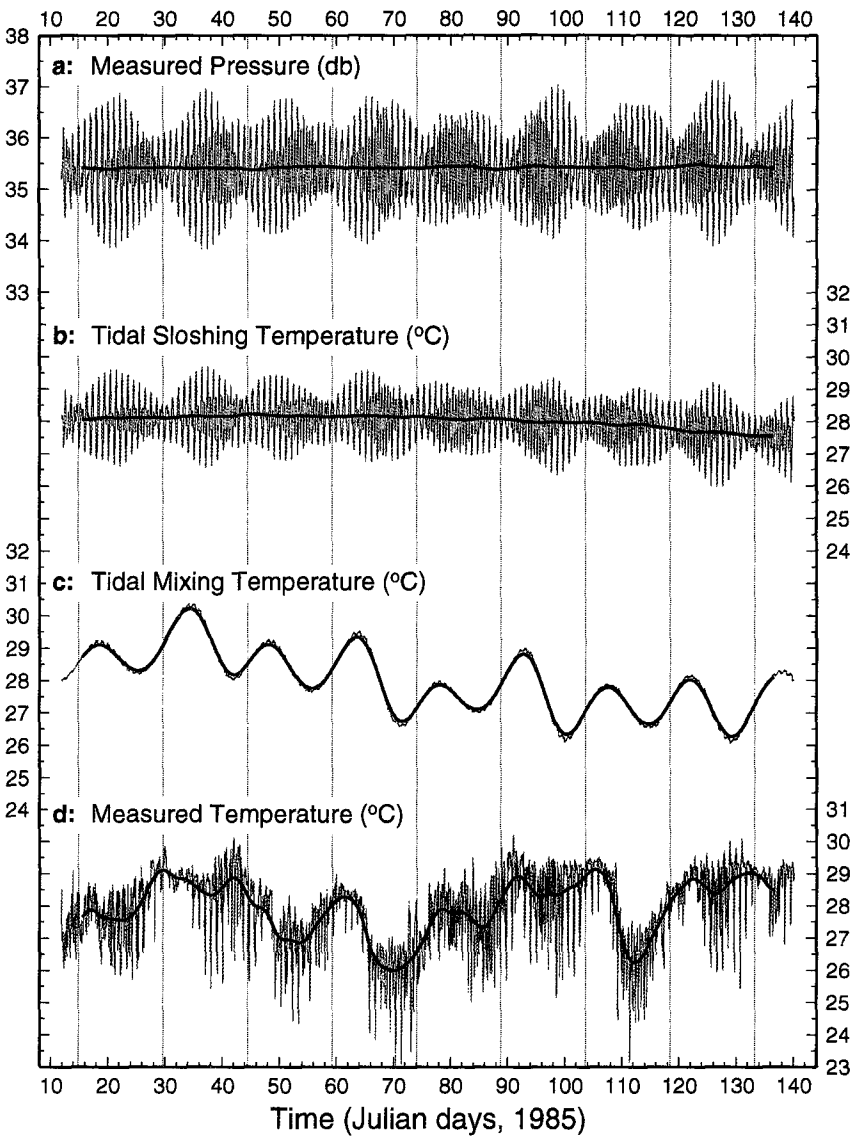

FIG. 5. The pressure (a) and temperature (d) time series data from the Lombok Strait tide gauge located at 8.7°S, 115.6°E (Murray and Arief 1990). The pressure time series is used to predict the tidal sloshing temperature (b) and the tidal mixing temperature (c). Atmospheric pressure has not been removed from the pressure records. A 7-day Gaussian average is drawn over each time series with a bold line. The timing of the fortnightly tidal cycle is marked by the dotted vertical lines.

a. Tidal sloshing parameterization

The first parameterization inspects for the effects of tidal sloshing. Tidal currents are envisioned to slosh water of different temperature back and forth with each tidal cycle, but without producing turbulence that would vertically mix the water column. The tidal currents advect water with an assumed linear horizontal temperature gradient across the sensor: ebb tidal currents may be expected to carry warm shelf water, and flood tidal currents carry cool off-shelf water. The change in temperature observed at the gauge is then just proportional to the changing speed and direction of the tidal currents,

$$\frac{dTe_{\text{slosh}}}{dt} = -c_1 v(t)_{\text{tidal}}.$$

The constant c_1 represents local thermal conditions and is assumed to equal 1°C s m^{-2} for utmost simplicity. Because the Lombok gauge did not include a current meter, the time derivative of the pressure time series

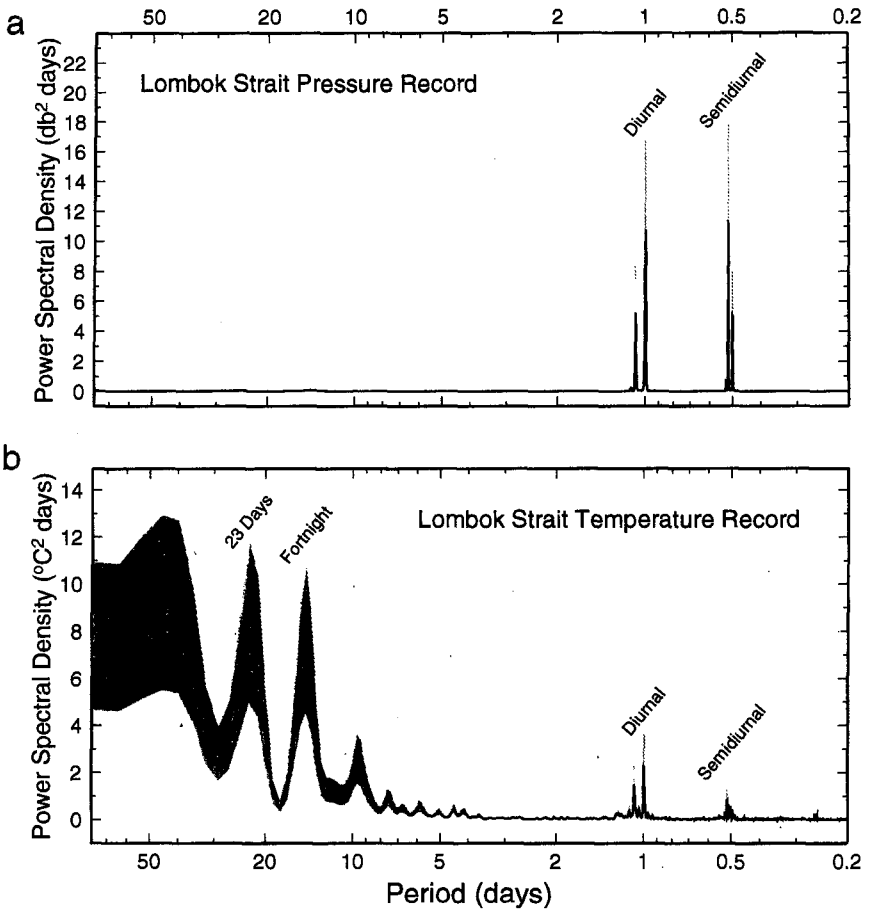

FIG. 6. The variance of the Lombok Strait pressure (a) and temperature (b) time series data distributed by period. Confidence intervals of 80% are illustrated by gray shading.

(with mean and trend removed) is used as a proxy for tidal currents.

The tidal sloshing parameterization is applied to the pressure time series in order to predict the possible temperature changes (Fig. 5b). An initial temperature of 28°C is used. As mentioned above, an associated linear temperature variation may be expected. Large spring tide temperature variations of about 3°C range are observed in both the predicted tidal sloshing temperature record and the measured temperature record. Because the tidal sloshing parameterization is linearly proportional to the pressure record, a spectral analysis of the tidal sloshing time series would reveal the same periodicities as does the pressure time series, though with a shift in phase.

A 7-day Gaussian filter overlays the tidal sloshing temperature record (Fig. 5b), which removes the diurnal, semidiurnal, and shallow-water tides and their fortnightly and monthly modulations. In contrast, the observed temperature record in Fig. 5d reveals a 7-day Gaussian filter temperature record rich in fortnightly modulation. This indicates that simple horizontal oscillation or sloshing of water with a linear horizontal temperature gradient cannot be the source of these observed temperature changes.

b. Tidal mixing parameterization

The second parameterization represents tidal induced vertical mixing. The many different nonlinear dynamics associated with turbulent mixing are parameterized most simply here by assuming that the square of the tidal current is proportional to the effect of turbulent vertical mixing on temperature (Pugh 1987; Pingree et al. 1978):

$$\frac{dTe_{\text{mix}}}{dt} = -c_2 v(t)^2_{\text{tidal}}.$$

It is envisioned that tidal mixing would lower SST as subsurface water is mixed into the surface layer, and that the cooling would be proportional to the intensity of the mixing. Both flood and ebb tidal speeds would act to cool SST, as the squared magnitude of the tidal current affects temperature. The constant, c_2, represents

the local thermal conditions and the efficiency of the tidal mixing; it is assumed to equal 1°C s m^{-2} for simplicity. The square of the time derivative of the pressure time series is used as a proxy for $v(t)^2_{\text{tidal}}$ with the mean and trend removed, and an initial temperature of 28°C is again assumed.

The pressure record is now used to predict the possible temperature changes from tidal mixing, and the result is a nearly pure fortnightly and monthly tidal signal (Fig. 5c). During spring tides the temperature of the water column is continuously cooled because both flood and ebb currents are larger than usual, increasing the amount of turbulent mixing. Correspondingly, during neap tides the water column continuously warms because both flood and ebb currents are smaller than usual, decreasing the amount of turbulent mixing.

The nonlinearity of the $v(t)^2_{\text{tidal}}$ calculation redistributed the tidal energy and produced new periodicities. When the principle semidiurnal lunar tide with period $T_{M_2} = 0.518$ day and principle semidiurnal solar tide with period $T_{S_2} = 0.5$ day are combined,

$$\cos\omega_{M_2}t + \cos\omega_{S_2}t,$$

they beat with a 14.8 day modulation. However, when the combination is squared, as it is in the $v(t)^2_{\text{tidal}}$ calculation, and reorganized using trigonometric functions (following Pugh 1987, page 110),

$$1 + 0.5\cos2\omega_{M_2}t + 0.5\cos2\omega_{S_2}t + \cos(\omega_{M_2} + \omega_{S_2})t + \cos(\omega_{S_2} - \omega_{M_2})t,$$

the mean is changed, three terms vary with periods of about 0.25 day, and the last term varies with a period of 14.8 days. The original semidiurnal terms are gone, and rather than a fortnightly modulation of the semidiurnal tides, there is now an explicit fortnightly constituent.

In addition, squaring the combination of the principle semidiurnal lunar tide with period $T_{M_2} = 0.518$ day and the semidiurnal larger elliptical lunar tide with period $T_{N_2} = 0.527$ day produces a new monthly constituent of 27.6 days. Another important constituent, 13.7 days, is produced by squaring the combination of the principle diurnal lunar tide with period $T_{O_1} = 1.076$ day and the principle diurnal lunar tide with period $T_{K_1} = 0.997$ day.

These new fortnightly and monthly constituents will not be removed by a weekly filter and, as such, the 7-day Gaussian average of the tidal mixing temperature time series in Fig. 5c preserves fortnightly and monthly tidal periods. The 7-day Gaussian average of the observed temperature record (Fig. 5d) also preserves a fortnightly cycle, though there is not an obvious monthly cycle in the record. From day 60 to 74 and from day 104 to 118 the observed fortnightly temperature cycle clearly corresponds with the tidal mixing fortnightly temperature cycle. The fortnightly range of the predicted tidal mixing temperature and the observed

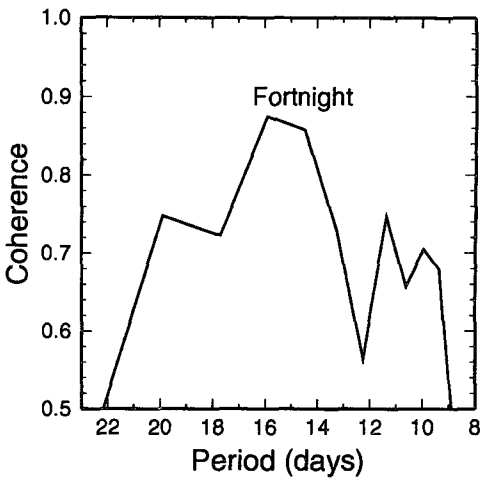

FIG. 7. The coherence of the Lombok Strait observed temperature time series and predicted tidal mixing temperature time series.

average temperature is about 3°C. In addition, the coherence (square root linear correlation coefficient as a function of period) at the fortnightly period is relatively high: 0.87 (Fig. 7).

Significant fortnightly and monthly tidal signals observed in the averaged temperature record and not in the averaged pressure record can be attributed to nonlinear tidal mixing. In this way, the pressure and temperature records of the Lombok Strait suggest that tidal mixing strongly influences the Lombok Strait temperature at the fortnightly tidal period. While other nonlinear tidal dynamics such as tidal rectification (Loder 1980) may effect fortnightly and monthly temperatures, those processes also mix the water column. Consequently, we do not attempt to distinguish between various tidal phenomena.

5. CAC satellite SST data

The Climate Analysis Center (CAC) optimal interpolation weekly SST data product combining in situ and AVHRR (Advanced Very High Resolution Radiometer) satellite data with one-degree grid resolution (Folland et al. 1993; Reynolds and Marsico 1993) is analyzed for SST tidal signatures in the Indonesian seas. The temporal length and geographical breadth of the satellite time series provide extensive coverage of the Indonesian seas. The time series include the November 1981 to April 1995 CAC data, and the spectral analysis results are produced from the January 1990 to April 1995 CAC data in order to avoid the change in the midweek definition. The CAC data processing removes high-frequency energy from the temperature values, by producing a weekly averaged data product. This minimizes aliasing of high-frequency energy into the spectral analysis results that are calculated for periods of 14 days and longer. While the weekly temporal resolution of the

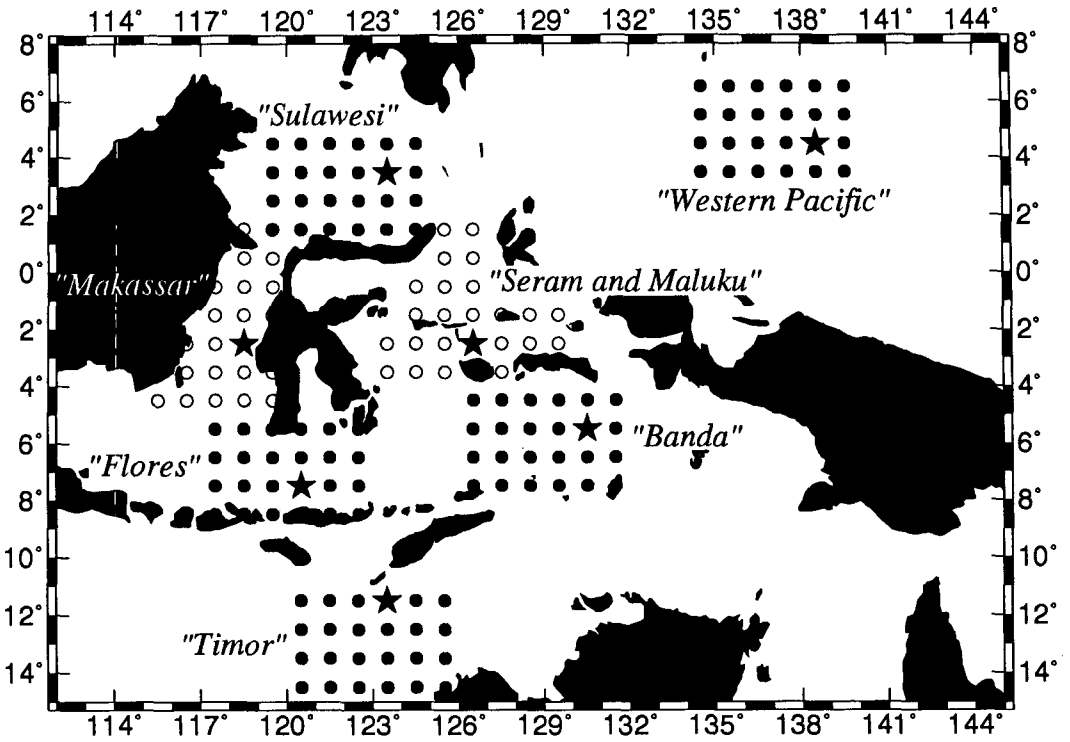

FIG. 8. Map of the Indonesian Seas showing the locations of the CAC optimal interpolation of in situ and AVHRR satellite sea surface temperature time series data used in Fig. 9 (stars) and in Fig. 10 (circles).

dataset limits the spectral analysis to periods greater than 14 days, it was demonstrated in section 4 that significant changes in SST due to tidal-induced vertical mixing processes are only expected at low-frequency tidal periods. The fortnightly constituent at 13.7 days will not be resolved by this analysis, but the fortnightly constituent at 14.8 days and all the monthly constituents will be resolved. Because the SST dataset is a weekly average, any significant fortnightly or monthly tidal signals in the SST time series can be attributed directly to tidal mixing rather than to modulations of the diurnal and semidiurnal tidal induced SST variation. However, aliasing and nontidal sources of energy may contribute to energy found at the tidal periods.

a. SST time series

Seven sample SST time series illustrate a typical SST record from the CAC dataset for each of the major Indonesian basins and the western Pacific Ocean (Figs. 8 and 9). The annual cycle is the most pronounced signal in the Indonesian SST with a 3°C annual range in the Makassar Strait and a 5°C annual range in the Banda Sea. The most striking feature in the SST is the cold July–August SST in the Banda Sea, with a similar signal mirrored in the Flores, Seram, and Timor Seas. The large decrease in the Banda Sea SST during July–August may be associated with shoaling of the thermocline during that season in response to regional wind-driven divergence of surface water (Wyrtki 1961). A shallower thermocline may amplify the cooling effects of vertical mixing on SST. Additionally, ocean–atmosphere heat flux factors, such as reduced "winter" solar radiation and the evaporative effects of the drier monsoonal winds from Australia during July–August may be expected to lower SST. The Northern Hemisphere Sulawesi Sea and western Pacific sites show cooler SST in January–February.

In the Banda Sea the July–August SST minimum vary by 2°C interannually, which may reflect El Niño variability. Colder than usual July–August SSTs occur in the El Niño years 1982, 1987, and 1992. Cooler than usual SSTs in the eastern Indonesian seas would contribute to the diminished atmospheric convection and associated drought conditions in Indonesia during El Niño.

b. SST power spectra

In order to investigate the periodicity of the changes in the Indonesian SST 24 neighboring SST time series were extracted from the CAC dataset for each basin (Fig. 8). Each SST time series was modified into a time series of the change in SST per week. A power spectral density estimate for each basin was calculated by, first, splitting each modified time series into two segments and averaging together their power spectral density es-

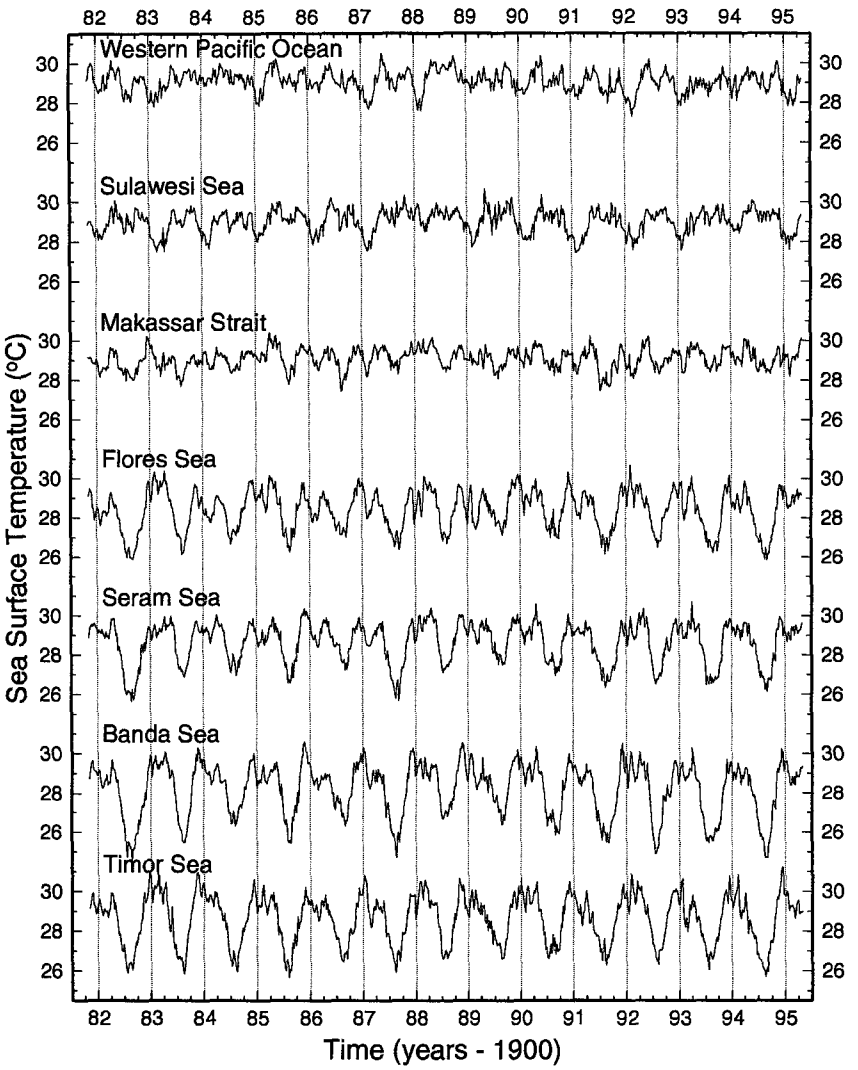

FIG. 9. One example of a satellite sea surface temperature time series for each basin. The temporal resolution is one week, and the positions of the time series are Western Pacific: 4.5°N, 138.5°E; Sulawesi: 3.5°N, 123.5°E; Makassar: 2.5°S, 118.5°E; Flores: 7.5°S, 120.5°E; Seram: 2.5°S, 126.5°E; Banda: 5.5°S, 130.5°E; and Timor: 11.5°S, 123.5°E.

timates. Then, the 24 neighboring power spectral density estimates for each basin were averaged together, and smoothed by a 5.8×10^{-8} s^{-1} Gaussian filter (Fig. 10). The power spectral density function describes how the variance of the data is distributed by frequency, and the averaging of the power spectral density estimates increases the confidence in the results and allows for differences in phases between locations.

The Banda Sea has the largest signals in the power spectral density plot (Fig. 10) with significant peaks at the fortnightly and monthly tidal periods, and at periods of 23, 60, 183, and 365 days. The Seram, Maluku, and Timor Seas also have large monthly peaks, and the Seram and Maluku Seas have large fortnightly peaks. The Sulawesi Sea, Makassar Strait, and Flores Sea reveal significant fortnightly and monthly tidal signals, but they are smaller than those in the eastern seas. As mentioned above, tidal-induced vertical mixing may be expected to produce fortnightly and monthly periodicities in the SST as colder water is mixed up to the surface during periods of stronger tidal mixing. The differences between the basin spectra can be caused by differences in the local tides, stratification, topography, and proximity to internal tide generation sites. The other distinct peaks in the spectra may also reflect tidal mixing, but those periods are not necessarily unique to tides. For example, the 60-day periodicity may be a harmonic of the monthly tidal signal, or it may reflect

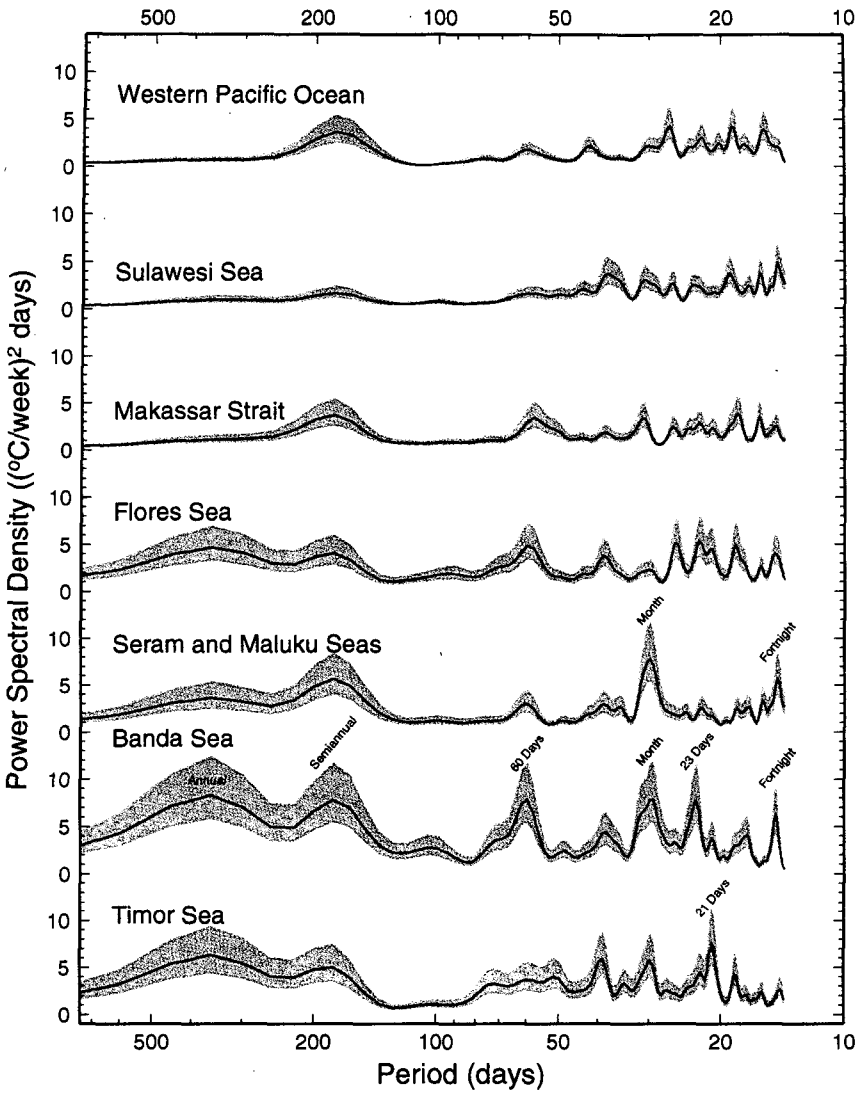

FIG. 10. The variance of the weekly change in sea surface temperature distributed by period for each basin (Fig. 8). Twenty-four neighboring power spectral density estimates of the weekly change in sea surface temperature were averaged together and then smoothed to form one robust estimate for each basin. Confidence intervals of 99% are illustrated by gray shading.

the 30–60 day Madden–Julian atmospheric oscillation (Weickmann and Khalsa 1990).

c. *Spatial pattern of fortnightly and monthly SST oscillations*

To view the spatial pattern of the SST time series at the fortnightly and monthly tidal periods, individual power spectral density estimates were calculated for every degree in the Indonesian seas and surrounding regions. The largest power within the fortnightly and monthly bandwidths is shaded and contoured in Figs. 11a and 11b. Larger values indicate SST changes from tidal mixing or just higher power at that period. The largest fortnightly power is observed in the Banda, Seram, Maluku, and Halmahera Seas. At the monthly period the largest power is observed in the Banda, Seram, and Timor Seas and the northwest Australian Shelf. The presence of both large fortnightly and monthly power in the Banda and Seram Seas (including the Lifamatola Sill) suggests that these signals are tidal because both the fortnightly and monthly periods are highly dependent on the same forcing, the M_2 tide. The TOPEX/POSEIDON satellite altimeter data reveals a large M_2 tide in the Sulawesi and Banda Seas (Mazzega and Berge 1994), supporting the SST results. Large tidal signals in the Banda Sea region are also predicted by a model of the flux of

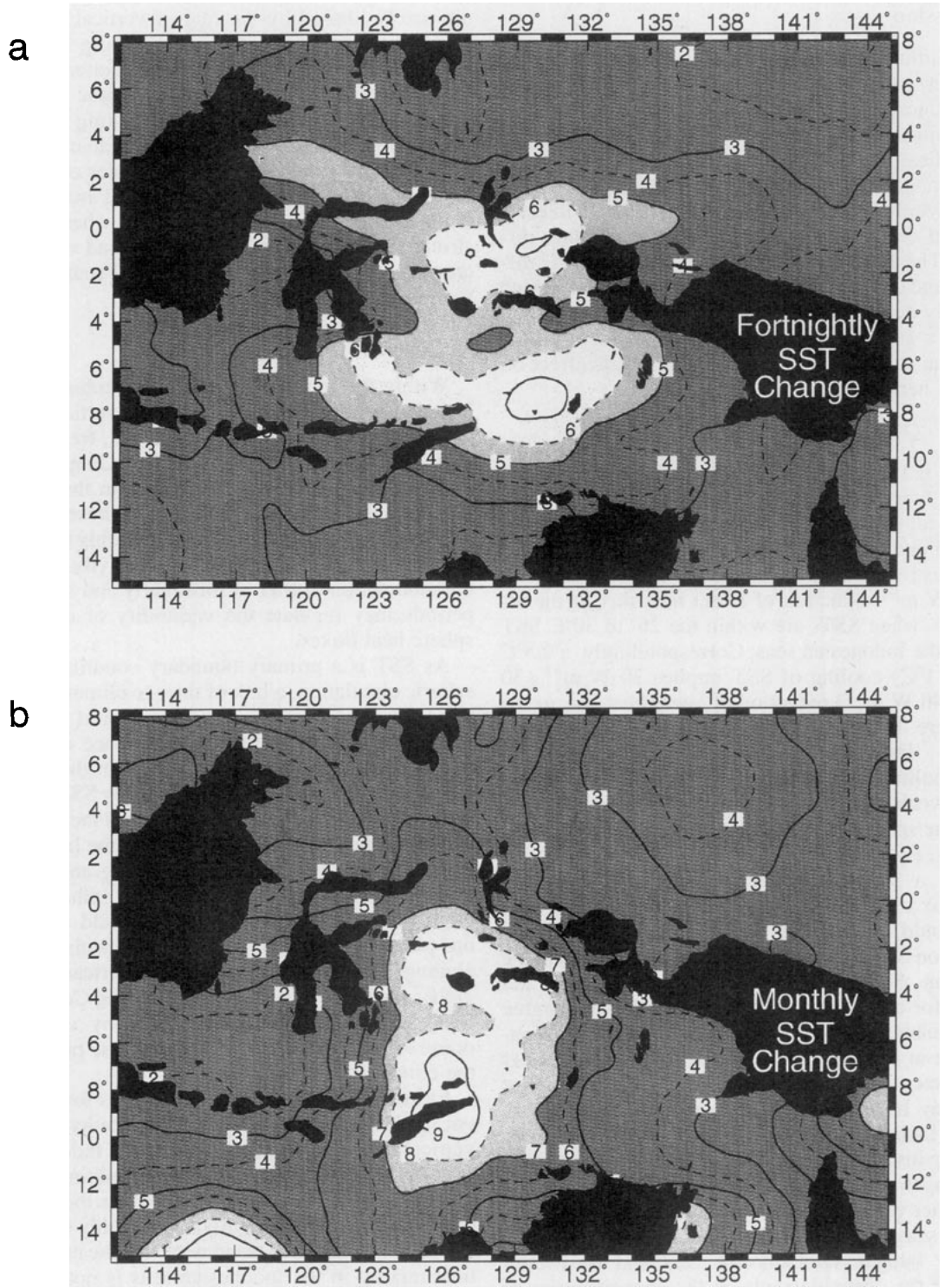

FIG. 11. Power spectral density estimates in the fortnightly (a) and monthly (b) bandwidths of the weekly change in sea surface temperature calculated for each one-degree square. The units of the contours are $(°C/wk)^2$ days.

tidal energy to mixing processes by topographically generated internal waves (Sjöberg and Stigebrandt 1992). In addition, the results correlate with the large thermocline oscillations and vertically mixed water properties observed in the eastern Indonesian Seas (Tables 1 and 2).

6. Discussion

Tidal influence on SST would be expected to have an impact on ocean–atmosphere heat fluxes. At the ocean–atmosphere boundary the net surface heat flux is determined by the balance of net radiation balance, sensible heat, and latent heat. The net longwave radiation term is not very sensitive to changes in SST. For a given wind speed, the sensible heat term is linearly dependent on the ocean–atmosphere temperature difference. The latent heat term also depends on this difference, and on the saturation humidity of the air, which is strongly dependent on SST at warm temperatures.

Using a standard bulk formula the change in heat flux Q due solely to a change in SST and its effect on the latent heat is

$$Q_2 - Q_1 = \rho_a C_E L |v| (q_{s_1} - q_{s_2}),$$

where ρ_a is the density of air, C_E is the exchange coefficient, L is the latent heat of vaporization, v is the wind speed, q_s is the saturation humidity; C_E is taken as 0.0015 and v is assumed to be 4 m s^{-1}. Using standard tables for q_s, a 0.25°C cooling of SST would result in a 10 W m^{-2} reduction of latent heat flux to the atmosphere, when SSTs are within the 26° to 30°C SST range of the Indonesian seas. Correspondingly, a 0.5°C (0.75°C, 1°C) cooling of SST implies 20 W m^{-2} (30 W m^{-2}, 40 W m^{-2}) reduction of latent heat flux to the atmosphere. In contrast, when SSTs are near 9°C, only 3.5 W m^{-2} less heat is fluxed to the atmosphere for a 0.25°C cooling of SST. The Lombok Strait temperature record reveals an average of 2.5°C cooler temperatures during one spring tide (near day 111 on Fig. 5d); consequently, even with a reduced 1 m s^{-1} wind speed for example, a substantial low-frequency ocean–atmosphere flux of 25 W m^{-2} is implied. The sensible heat fluxes would further amplify the dependence of total heat flux on SST changes. Therefore, oscillations in the Indonesian SST, at tidal periods, fortnightly and monthly for example, of only a few tenths of a degree will modulate the heat flux from the ocean to the atmosphere at these periods by many tens of watts per square meter. Such changes in ocean–atmosphere heat fluxes may have a significant equatorial atmospheric response including changes in convective activity due to the sensitivity of the equatorial atmosphere to small SST changes (Graham and Barnett 1987).

A further effect of the enhanced mixing within Indonesian seas may be related to the large-scale oceanic buoyancy budget. Globally the heat and freshwater storage of the ocean depends on the characteristics of convective water masses, but these are not independent of vertical mixing. Vertical mixing carries buoyancy into the deep ocean, compensating the water mass formation and making possible continued displacement of resident water by convection. In a steady-state ocean, oceanic convection cannot continue without the compensating effects of vertical mixing and is, therefore, ultimately limited by the rate of vertical mixing. The compensating effects of vertical mixing may be concentrated in some "active" regions. For example, most of the Indonesian Throughflow passes through the Banda Sea where strong vertical mixing modifies the thermocline by transferring surface heat and freshwater to deeper layers before the upper water column is exported to the Indian Ocean. Vertical mixing and its variations in the Indonesian region where there is a strong vertical gradient of buoyancy and vigorous tidal currents may play a key role in global-scale ocean ventilation.

7. Conclusions

Within the Indonesian seas, the combination of enhanced vertical mixing and strong vertical gradients will drive large vertical fluxes of heat, freshwater, and nutrients through the water column. Coupling of tidal dissipation and vertical mixing within the Indonesian seas suggests that the vertical flux of these ocean properties will vary at fortnightly and monthly tidal periods, possibly influencing primary productivity. In addition, the modulation of SST at fortnightly and monthly tidal periods may regulate the variability of ocean–atmosphere heat fluxes.

As SST is a primary boundary condition for atmospheric circulation, a link of tides to climate is a natural topic for speculation. Loder and Garrett (1978) suggested the possible climatic importance of tidally induced vertical mixing through SST. In the eastern Indonesian seas, tidal mixing influences SST and possibly ocean–atmosphere heat fluxes, and the throughflow carries the products of tidal mixing to the Indian Ocean. Consequently, variations in the timing and magnitude of tidal mixing have the potential to influence the regional and global climate system (Ffield 1994). Various phenomena have been associated with the tides including thunderstorm frequency, hurricanes, and the global surface temperature (Balling and Cerveny 1995; Best 1994). SST variations driven by variable tidal ocean mixing is a possible link of these phenomena to the climate system.

Evidence for tidal-induced mixing is found throughout the Indonesian seas, supporting the hypothesis that vertical mixing is enhanced within the Indonesian Seas by tidal mixing. The largest tidal mixing signatures away from the coasts are observed in the Seram and Banda Seas at the fortnightly and monthly tidal periods. However, the physics responsible for the enhanced vertical mixing in the Indonesian seas is not included in any global circulation models. It may be important to do so—even for climate models—as the products of enhanced vertical mixing in the Indonesian seas may modulate equatorial ocean–atmosphere and interocean heat, freshwater, and carbon fluxes.

Acknowledgments. The authors thank Dr. Steve Murray for providing the Lombok Strait pressure and tem-

perature data, Dr. J. M. Van Aken for the *Snellius-II* data reports, Dr. Richard Reynolds for the satellite SST data, and the reviewers for their constructive comments. Our collaboration with Dr. A. Gani Ilahude and the support of the Indonesian oceanography community led to the successful joint U.S.–Indonesian ARLINDO Mixing program. This work was supported by the Office of Naval Research Contract N00014-90-J-1233 and National Science Foundation Grant OCE-9302607.

REFERENCES

Balling, R. C., and R. S. Cerveny, 1995: Influence of lunar phase on daily global temperatures. *Science,* **267,** 1481–1483.

Best, C. H., 1994: Observation of a monthly variation in global surface temperature data. *Geophys. Res. Lett.,* **21,** 2369–2372.

Broecker, W. S., W. C. Patzert, J. R. Toggweiler, and M. Stuiver, 1986: Hydrography, chemistry, and radioisotopes in the Southeast Asian basins. *J. Geophys. Res.,* **91,** 14 345–14 353.

Cartwright, D. E., and R. D. Ray, 1989: New estimates of oceanic tidal energy dissipation from satellite altimetry. *Geophys. Res. Lett.,* **16,** 73–76.

Ffield, A. L., 1994: Vertical mixing in the Indonesian Seas. Ph.D. thesis, Columbia University, 150 pp.

——, and A. L. Gordon, 1992: Vertical mixing in the Indonesian Seas. *J. Phys. Oceanogr.,* **22,** 184–195.

Folland, C. K., R. W. Reynolds, M. Gordon, and D. E. Parker, 1993: A study of six operational sea surface temperature analyses. *J. Climate,* **6,** 96–113.

Godin, G., 1972: *The Analysis of Tides.* University of Toronto Press, 264 pp.

Gordon, A. L., 1995: When is appearance reality? A comment on why does the Indonesian throughflow appear to originate from the North Pacific. *J. Phys. Oceanogr.,* **25,** 1560–1567.

——, A. Ffield, and A. G. Ilahude, 1994: Thermocline of the Flores and Banda Seas. *J. Geophys. Res.,* **99,** 18 235–18 242.

Graham, N. E., and T. P. Barnett, 1987: Sea surface temperature, surface wind divergence, and convection over tropical oceans. *Science,* **238,** 657–659.

Ilahude, A. G., and A. L. Gordon, 1996: Thermocline stratification within the Indonesian Seas. *J. Geophys. Res.,* in press.

Jonker, P. J., J. Punjanan, and H. M. van Aken, 1986: *Data report on a mooring station in Strait Lifamatola.* Tech. Rep. R 86-13, 31 pp. [Available from Institute for Meteorology and Oceanography, State University Utrecht, 5 Princetonplein, 3584 CC Utrecht, the Netherlands.]

Loder, J. W., 1980: Topographic rectification of tidal currents on the sides of Georges Bank. *J. Phys. Oceanogr.,* **10,** 1399–1416.

——, and C. Garrett, 1978: The 18.6-year cycle of sea surface temperature in shallow seas due to variations in tidal mixing. *J. Geophys. Res.,* **83,** 1967–1970.

Mazzega, P., and M. Bergé, 1994: Ocean tides in the Asian semienclosed seas from TOPEX/POSEIDON. *J. Geophys. Res.,* **99,** 24 867–24 881.

Mihardja, D. K., 1991: Energy and momentum budget of the tides in Indonesian waters. Ph.D. thesis, Institut fur Meereskunde, Hamburg, 183 pp.

Miller, G. R., 1966: The flux of tidal energy out of the deep oceans. *J. Geophys. Res.,* **71,** 2485–2489.

Murray, S. P., and D. Arief, 1990: Characteristics of circulation in an Indonesian archipelago strait from hydrography, current measurements and modeling results. *The Physical Oceanography of Sea Straits,* L. J. Pratt, Ed., Kluwer Academic, 3–23.

New, A. L., 1988: Internal tidal mixing in the Bay of Biscay. *Deep-Sea Res.,* **35,** 691–709.

——, and R. D. Pingree, 1990: Evidence for internal tidal mixing near the shelf break in the Bay of Biscay. *Deep-Sea Res.,* **37**(12A), 1783–1803.

Padman, L., and T. M. Dillon, 1991: Turbulent mixing near the Yermak plateau during the coordinated eastern Arctic experiment. *J. Geophys. Res.,* **96,** 4769–4782.

Pingree, R. D., and A. L. New, 1991: Abyssal penetration and bottom reflection of internal tidal energy in the Bay of Biscay. *J. Phys. Oceanogr.,* **21,** 28–39.

——, P. M. Holligan, and G. T. Mardell, 1978: The effects of vertical stability on phytoplankton distributions in the summer on the northwest European shelf. *Deep-Sea Res.,* **25,** 1011–1028.

Pugh, D. T., 1987: *Tides, Surges, and Mean Sea-Level, a Handbook for Engineers and Scientists.* Wiley & Sons, 472 pp.

Reynolds, R. W., and D. C. Marsico, 1993: An improved real-time global sea surface temperature analysis. *J. Climate,* **6,** 114–119.

Sandstrom, H., and N. S. Oakey, 1995: Dissipation in internal tides and solitary waves. *J. Phys. Oceanogr.,* **25,** 604–614.

Schott, F., 1977: On the energetics of baroclinic tides in the North Atlantic. *Ann. Geophys.,* **33,** 41–61.

Sjöberg, B., and A. Stigebrandt, 1992: Computations of the geographical distribution of the energy flux to mixing processes via internal tides and the associated vertical circulation in the ocean. *Deep-Sea Res.,* **39,** 269–291.

Van Aken, H. M., J. Punjanan, and S. Saimima, 1988: Physical aspects of the flushing of the East Indonesian basins. *Neth. J. Sea Res.,* **22,** 315–339.

Weickmann, K. M., and S. J. S. Khalsa, 1990: The shift of convection from the Indian Ocean to the western Pacific Ocean during a 30–60 day oscillation. *Mon. Wea. Rev.,* **118,** 964–978.

Wesson, J. C., and M. C. Gregg, 1994: Mixing at Camarinal Sill in the Strait of Gibraltar. *J. Geophys. Res.,* **99,** 9847–9878.

Wunsch, C., 1975: Internal tides in the ocean. *Rev. Geophys. Space Phys.,* **13,** 167–182.

Wyrtki, K., 1961: *Physical oceanography of the Southeast Asian waters.* NAGA Report, Vol. 2, Scripps Institute of Oceanography, 195 pp.